ACS APPLIED MATERIALS & INTERFACES

Research Article

www.acsami.org

Microstructural Control over Soluble Pentacene Deposited by Capillary Pen Printing for Organic Electronics

Wi Hyoung Lee,[†] Honggi Min,[‡] Namwoo Park,[‡] Junghwi Lee,[‡] Eunsuk Seo,[‡] Boseok Kang,[§] Kilwon Cho,[§] and Hwa Sung Lee*[,‡]

[†]Department of Organic and Nano System Engineering, Konkuk University, Seoul 143-701, Korea

[‡]Department of Chemical & Biological Engineering, Hanbat National University, Daejeon 305-719, Korea

[§]Department of Chemical Engineering, Pohang University of Science and Technology, Pohang 790-784, Korea

ABSTRACT: Research into printing techniques has received special attention for the commercialization of cost-efficient organic electronics. Here, we have developed a capillary pen printing technique to realize a large-area pattern array of organic transistors and systematically investigated self-organization behavior of printed soluble organic semiconductor ink. The capillary pen-printed deposits of organic semiconductor, 6,13-bis(triisopropylsilylethynyl) pentacene (TIPS_PEN), was well-optimized in terms of morphological and microstructural properties by using ink with mixed solvents of chlorobenzene (CB) and 1,2-dichlorobenzene (DCB). Especially, a 1:1 solvent ratio results in the best transistor performances. This result is attributed to the unique evaporation characteristics of the TIPS_PEN deposits where fast evaporation of CB induces a morphological evolution at the initial printed position, and the remaining DCB with slow evaporation rate offers a favorable crystal evolution at the pinned position. Finally, a large-area transistor array was facilely fabricated by drawing organic electrodes and active layers with a versatile capillary pen. Our approach provides an efficient printing technique for fabricating large-area arrays of organic electronics and further suggests a methodology to enhance their performances by microstructural control of the printed organic semiconducting deposits.

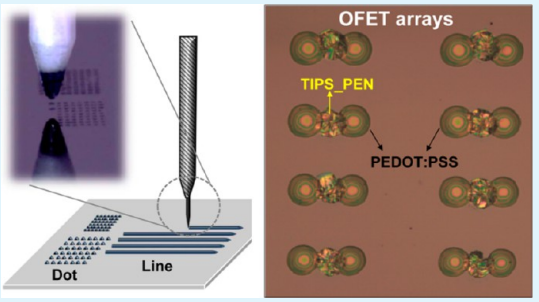

KEYWORDS: *capillary pen printing, organic field-effect transistors, soluble pentacene, capillary action, organic electronics*

1. INTRODUCTION

Organic field-effect transistors (OFETs) have received much attention for their potential uses in flexible electronics.[1−10] OFET devices now yield performances comparable to those of their inorganic counterparts; however, several barriers remain before OFETs may be commercialized. One such barrier is the development of printing techniques that can be used for the low-cost mass production of OFETs.[11−15] Although commercially available printing techniques, such as inkjet printing, are relatively cost-efficient, certain technical problems must be addressed before these techniques may be applied in a commercial capacity.[12,16−20] Inkjet printing techniques are frequently hindered by nozzle clogging, pattern inaccuracies, and nonuniform layer deposition. Although nozzle clogging can be reduced by adjusting the ink formulation,[20,21] this problem significantly disrupts sequential printing processes. Noncontact inkjet printing typically leads to the unwanted deposition of materials at a defined position. These depositions reduce the electrical performance of the printed material and degrade the reproducibility of the patterned devices. Contact printing techniques provide alternative routes for printing that avoid these types of problems.[22]

Several contact printing techniques have been developed for printing active components in OFETs. Among these techniques, soft lithography and roll-to-roll printing techniques have shown promise in the context of micro- and nanoscale patterning of solution-processed materials. Soft lithography uses an elastomeric stamp, polydimethylsiloxane (PDMS), which is amenable to repeated processing uses and provides a reusable mold.[23] Notwithstanding the apparent advantages of soft lithography, the technique is limited to certain commercial purposes due to problems involved in scaling up the printing technique. Other issues that must be addressed in order to obtain well-defined patterns are PDMS mold swelling in the presence of organic solvents and control over the adhesion between the inks and both the PDMS mold and the substrate.[22,24] Continuous roll-to-roll printing techniques provide alternative approaches to high-speed large-area patterning with excellent throughput.[2,25−29] Recently, a continuous printing technique was used to prepare patterns several micrometers in size; however, roll-to-roll printing techniques encounter problems if it is necessary to position multistacked patterns and modify pattern shapes during operation.[30] A new contact printing technique is required for the commercialization of OFETs.

The commercially available capillary pen offers an alternative printing technique. A capillary pen is a convenient printing apparatus for soluble organic materials, such as organic

Received: May 6, 2013
Accepted: July 29, 2013
Published: July 29, 2013

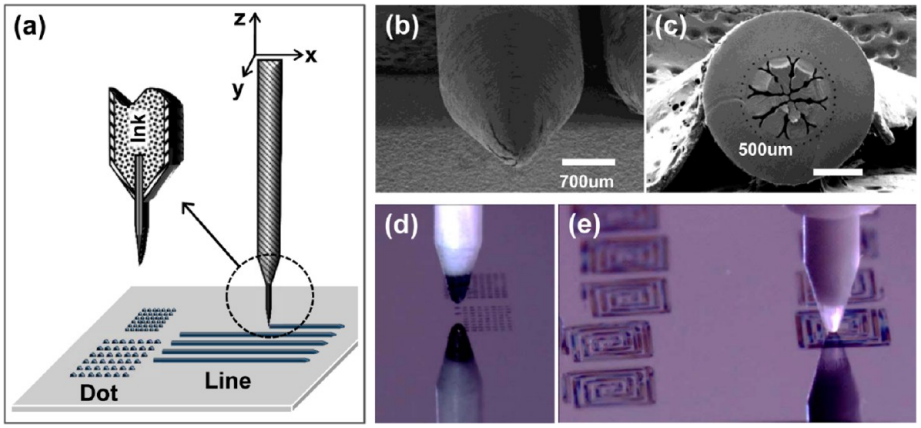

Figure 1. (a) Schematic diagram showing a capillary pen system. The process of drawing with the pen resulted in ink ejection from the nib to form dot and line patterns on the substrate. (b) SEM image of the nib. (c) Cross-sectional image of the nib. (d and e) CCD camera images of the dot and line patterns, respectively, drawn with the pen.

semiconductors and conductors. Printing is accomplished through direct contact between the pen and the target substrate. The pen-based printing process is simple and versatile and is not significantly influenced by external conditions, such as the ambient temperature or air flow. Capillary pen printing is not restricted in terms of the pattern shapes, and dots, lines, and faces may be printed using capillary pens. Patterns may be formed rapidly and accurately using a capillary pen. Here, we used a capillary pen to print organic semiconductor ink, and we systematically investigated the dependence of the pattern formed by a soluble organic semiconductor on the solution properties, including the solvent evaporation rate and the surface tension. 6,13-Bis((triisopropylsilylethynyl) pentacene (TIPS_PEN) was used as a model organic semiconductor because this material provides an excellent and well-characterized electrical performance, particularly in the context of OFET applications.[20,31−34] The crystalline microstructures and film morphologies of the TIPS_PEN deposits were analyzed by two-dimensional grazing incidence X-ray diffraction (2D GIXD), optical microscopy (OM), and field-emission scanning electron microscopy (FE-SEM). The relationships between these characteristics and the electrical performances of the resulting FET devices were also investigated.

2. EXPERIMENTAL SECTION

Materials and Device Fabrication. A commercially available capillary nib was obtained from a water-based pen (Monami, plus pen 3000), after removing the commercial ink from the nib. The nib was cleaned by applying more than five washing cycles, each involving an ethanol rinse and sonication in a distilled water bath, and then dried using compressed N_2 gas. The nib was combined with a homemade pen holder consisting of an ink reservoir and a pen extender fabricated from Teflon and Al, respectively. The combined capillary pen was then mounted on a home-built control system with a three-axis positioning motor and a charge-coupled device (CCD) camera. 6,13-Bis((triisopropylsilylethynyl) pentacene (TIPS_PEN) from Aldrich was dissolved in a variety of solvents (i.e., hexane (HEX), octane (OCT), toluene (TOL), chlorobenzene (CB), 1,2-dichlorobenzene (DCB), and 1,2,4-trichlrobenzene (TCB)) to prepare the pen inks. The total concentration of TIPS_PEN was adjusted to 3 wt %. The TIPS_PEN inks were then introduced into the reservoir and were ejected from the nib by capillary action. During the printing process, the moving speed of the nib was 5 mm/min. When the nib touched the substrate surface, we immediately stopped the approach of the nib toward the substrate to avoid surface damage as much as possible. The contact between the nib and the substrate was maintained for approximately 0.5 s, and the nib was quickly removed from the substrate after forming TIPS-PEN droplet. All drawing process were observed and controlled by a CCD camera in real time. The droplet dried at atmospheric condition (temperature 20 °C, relative humidity 30%) without any external forces.

The FET devices were built on 300 nm thick SiO_2/Si substrates. Highly doped Si served as the gate electrode and a thermally grown 300 nm thick SiO_2 layer served as the gate dielectric. The source/drain (S/D) electrodes were defined by thermally evaporating Au (30 nm)/Ti (3 nm) onto the SiO_2/Si substrate. Alternatively, poly(3,4-ethylenedioxythiophene):poly(styrenesulfonate) (PEDOT:PSS) S/D electrodes were fabricated using a capillary pen. Hexamethyldisilazane (HMDS) from Aldrich was coated onto the SiO_2/Si substrate by spin-casting to modify the SiO_2 surface.[35] Finally, TIPS-PEN inks were selectively deposited onto the channel region of the FET devices using the capillary pen.

Characterization. The nib of the capillary pen was characterized by FE-SEM (Hitachi S-4200). The morphologies of the deposits were examined by OM (Nikon Eclipse80i) and SEM imaging. The molecular orientations of the TIPS-PEN films were examined by 2D GIXD measurements collected at the Pohang Accelerator Laboratory (PAL) of Korea. The electrical properties of the FET devices were measured under N_2 flow conditions using Keithley 2363A source measure units.

3. RESULT AND DISCUSSION

Figure 1a shows a schematic diagram of the capillary pen system. The system provided an efficient patterning method for fabricating low-cost large-area organic electronics. The capillary pen was combined with an *xyz*-axis position controller to draw designed patterns with a high degree of control over the interval and size. Ink could be ejected via capillary action from the end of the nib, which had been obtained from a commercially available marker pen. An SEM image of the nib end, which included several capillary tubes, is shown in Figure 1b. The narrow tubes ran along the body of the nib, as shown in the cross-sectional SEM image (Figure 1c). Ink passing through the capillary tubes is concentrated at the end of the nib and is finally ejected from the nib, thereby drawing a pattern onto the target surface. Figure 1d and e show captured CCD camera images of dot and line patterns, respectively, prepared from the TIPS_PEN ink. The results demonstrate the usefulness and efficiency of the capillary pen system for patterning organic materials.

The effects of the solvent on the morphological and structural properties of the TIPS_PEN deposits were examined by employing solvents with different boiling points (BPs): toluene

Table 1. Physical Properties of the Solvents at Room Temperature (20 °C)

	TOL	CB	DCB	TCB
boiling point (deg)	110.6	131.7	180.5	214.4
surface tension (mN m^{-1})	28.5	33.3	36.7	39.1
average field-effect mobility (max)	0.006	0.014 (0.029)	0.034 (0.086)	
standard deviation	0.0033	0.0054	0.0206	

	HEX	OCT	CB(3):DCB(1)	CB(2):DCB(1)	CB(1):DCB(1)
boiling point	68.7	125.7			
surface tension[a]	18.5	21.6	34.1	34.4	35.0
average field-effect mobility (max)			0.049 (0.076)	0.054 (0.081)	0.060 (0.085)
standard deviation			0.0138	0.0142	0.0198

[a]Surface tensions of the mixed solvents were calculated based on a linear approximation.

(TOL), chlorobenzene (CB), 1,2-dichlorobenzene (DCB), and 1,2,4-trichlorobenzene (TCB). The physical properties of the solvents are summarized in Table 1. Figure 2 shows polarized optical microscopy (POM) images of the TIPS_PEN dots (with a dot-to-dot distance of 300 μm) prepared using the capillary pen system. Prior to patterning with the capillary pen, the surface energy of the substrate was tuned to be relatively hydrophobic (a surface energy of 45 mJ·m^{-2}) by treating the SiO_2/Si substrate with hexamethyldisilazane (HMDS).[35] The morphological properties of the TIPS_PEN deposits were found to be closely related to the solvent evaporation rate (and the BP). TOL, the solvent with the highest evaporation rate and the lowest surface tension, yielded deposits that did not form an exact dot shape because solvents with a low surface tension preferentially spread the droplet over the surface. Rapidly evaporating solvents produced irregularly shaped deposits. On the other hand, solvents with high BPs, such as CB, DCB, and TCB, yielded dot-shaped TIPS_PEN deposits. Interestingly, the pattern size decreased with increasing solvent BP because the slowly evaporating solvents permitted disruption of the solvent pinning at the contact line, and the high surface tension DCB or TCB solvents induced the contact line to recede.[35,36] Thus, the droplets formed from DCB or TCB resulted in shifts in the contact line toward the central region of the droplet.

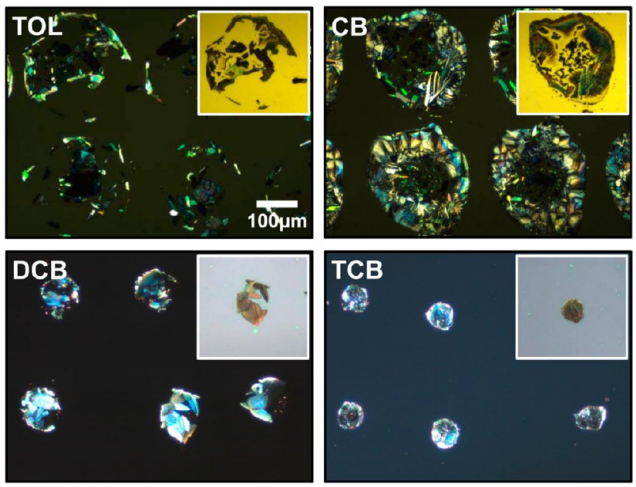

Figure 2. Polarized optical microscopy (POM) images of the TIPS_PEN dots prepared from various solvents: toluene (TOL), chlorobenzene (CB), 1,2-dichlorobenzene (DCB), 1,2,4-trichlorobenzene (TCB). The insets show OM images collected without a cross-polarizer.

Figure 2 confirmed that the optical contrast in the POM images became brighter as the solvent BP increased. This indicated an increase in the crystalline order on the micrometer scale as the solvent evaporation rate decreased. The outer regions of the TIPS_PEN deposits formed from CB were brighter than the central region. The TIPS_PEN deposits formed from TCB, however, did not display significant birefringence differences upon illumination. This result suggests that the TIPS_PEN deposit formed from TCB may provide better active layers in OFETs than TIPS_PEN deposits formed from CB or DCB. Note that a high crystallinity and morphological uniformity in an active layer can increase the field-effect mobility of an OFET.[31,37] Nevertheless, FET properties were not observed from the deposit formed from TCB (Table 1) due to the inaccuracies of the deposit (Figure 2). The positions of TIPS_PEN deposits formed from TCB deviated significantly from their intended positions because the contact line receded irregularly due to the extremely slow solvent evaporation rate and the high solvent surface tension. Deposits formed from DCB also displayed positioning problems, although these problems were not as serious as those observed in the TCB case. The relationship between the deposit microstructure and the OFET device performance was investigated by fabricating 29 transistors and measuring their electrical properties under identical conditions. As the solvent BP increased, the field-effect mobility of the resulting FET device increased in the order of TOL (0.006 cm^2 V^{-1} s^{-1}), CB (0.014 cm^2 V^{-1} s^{-1}), and DCB (0.034 cm^2 V^{-1} s^{-1}), as shown in Table 1. These results are consistent with the observed increase in the optical contrast of the TIPS_PEN deposits in the POM images. Interestingly, the standard deviation of the field-effect mobility also increased as solvent was changed from CB (±0.0054 cm^2 V^{-1} s^{-1}) to DCB (±0.0206 cm^2 V^{-1} s^{-1}). The dispersion in the mobility values arose partly from the problems of deposit positioning observed with the DCB solvent. Large crystals in the DCB deposits also contributed to the large variations in the field-effect mobility. This type of performance variability is typically reported in FETs prepared with organic single crystals, in which film uniformity and crystal connections were not guaranteed.[38,39] Further increases in both the mobility value and uniformity can be achieved by manipulating the solvent. To this end, we used mixed solvents to finely control the morphological and structural properties of the TIPS_PEN deposits prepared using the capillary pen system.

Figures 3 and 4 show POM images of the TIPS_PEN deposits prepared using solutions of mixed solvents. CB was used as the main solvent and various solvents (HEX, OCT, DCB) were added to prepare the pen ink. The concentration of TIPS_PEN in the solution was fixed to 3 wt %. The addition of HEX or OCT induced the TIPS_PEN deposits to become concentrated in an outer ring of the deposit (Figure 3) due to the coffee stain effect. Outward convective flow in a pinned

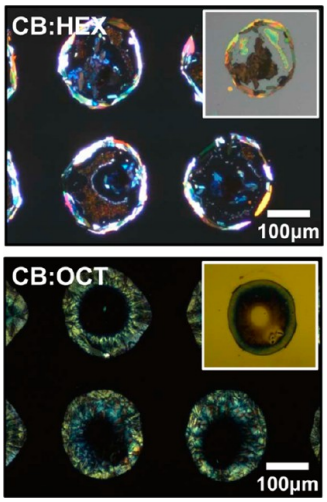

Figure 3. Polarized optical microscopy (POM) images of the TIPS_PEN dots prepared from mixed solvents hexane (HEX) and octane (OCT). The insets show OM images collected without a cross-polarizer.

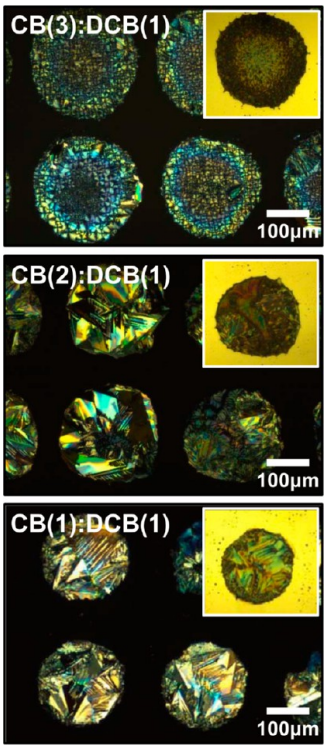

Figure 4. Polarized optical microscopy (POM) images of the TIPS_PEN dots prepared from CB and DCB mixed solvents with different solvent ratios. The insets show OM images collected without a cross-polarizer.

droplet can induce the TIPS_PEN molecules to move toward the pinned edge.[17,40] Coffee stain effects occur only when the solvent evaporation rate is relatively high and evaporation proceeds at the pinned edge. Note that the boiling point of the added solvent (HEX or OCT) was lower than that of CB. The evaporation processes of the CB/HEX or CB/OCT solvent mixtures contrasted with the processes observed using DCB or TCB (Figure 2), in which the solvent evaporation rate was low and the contact line receded during solvent evaporation. No FET characteristics were observed in the devices fabricated using TIPS_PEN deposits prepared from a mixed solvent consisting of CB and HEX (or OCT) because TIPS_PEN did not deposit in the center region, and the crystals were disconnected.

The solvent evaporation rate was further adjusted by adding DCB, which has a high BP. Figure 4 shows the POM images of the TIPS_PEN deposits prepared using the mixed CB/DCB solutions. The DCB mixing ratio was varied to examine the effects of DCB on the evaporation characteristics of the capillary pen-deposited droplet. As the DCB content increased, the crystal coverage increased (Figure 4). Although TIPS_PEN crystals were not observed at the center region of the deposit prepared from CB, crystals were detected over the full deposition areas in droplets deposited using the mixed CB and DCB solvents. The crystal size increased as the DCB content increased. The CB(3):DCB(1) mixture yielded a high number of nucleation sites for crystal formation, and a myriad of small TIPS_PEN crystals formed. As the DCB ratio was increased further, the nucleation number decreased, thereby increasing the size of the resultant (fewer) crystals. These results could be explained in terms of the evaporation characteristics of the mixed CB and DCB solvents. The CB evaporated first with a relatively rapid evaporation rate. During this stage, the contact line of a droplet remained pinned at the initial contact line position. The remaining TIPS_PEN solution became more concentrated, and the crystallization of the deposit progressed continuously with the assistance of the DCB remaining in the droplet. The slow solvent evaporation rate of the remaining DCB provided sufficient time for the TIPS_PEN molecules to self-organize, resulting in a deposit with a high coverage of large crystals. That is, the fast evaporation of the CB helps to induce the pinning of the droplet at the initial printed position, and the remaining the DCB with slow evaporation offers a favorable crystal evolution in the TIPS_PEN deposits.

Figure 5a shows representative transfer characteristics of the FET devices prepared from the TIPS_PEN deposits fabricated using the capillary pen with a mixed CB/DCB solvent. Bottom-contact FET devices were fabricated by direct deposition of a TIPS_PEN film on the channel regions between the Au source/drain electrodes. The transfer curves in Figure 5a show on/off current ratios exceeding 10^7 for all TIPS_PEN devices, and the turn-on voltages of the devices were near 0 V. Only the on-current varied, whereas the off-current, threshold voltage, and gate leakage current remained unchanged. The transfer characteristics were used to calculate the field-effect mobility in the saturation regime using the relationship $I_{DS} = C_i \mu W (V_{GS} - V_{th})^2/2L$, where W and L are the channel width and length, respectively, C_i is the specific capacitance of the gate dielectric, and μ is the field-effect mobility. The device-to-device reproducibility of the TIPS_PEN FETs fabricated by the capillary pen approach was examined by measuring the field-effect mobilities of 29 TIPS_PEN transistors, as summarized in Figure 5b and Table 1. The average field-effect mobilities (calculated in the saturation regime) as a function of the DCB ratio are also shown in Figure 6. The average field-effect mobilities of the devices increased with increasing DCB content. The highest average mobility of 0.06 $cm^2\ V^{-1}\ s^{-1}$ was obtained for the CB(1):DCB(1) case, with a standard deviation of 0.0198 $cm^2\ V^{-1}\ s^{-1}$. This value was much higher than that achieved for the pure DCB solvent. Abrupt receding of the contact line, observed in droplets deposited using the DCB solvent, triggered droplet shrinkage, resulting in TIPS_PEN deposits with irregular dot patterns and relatively small crystal sizes. In the mixed CB and DCB solvents, however, CB evaporated first, and the

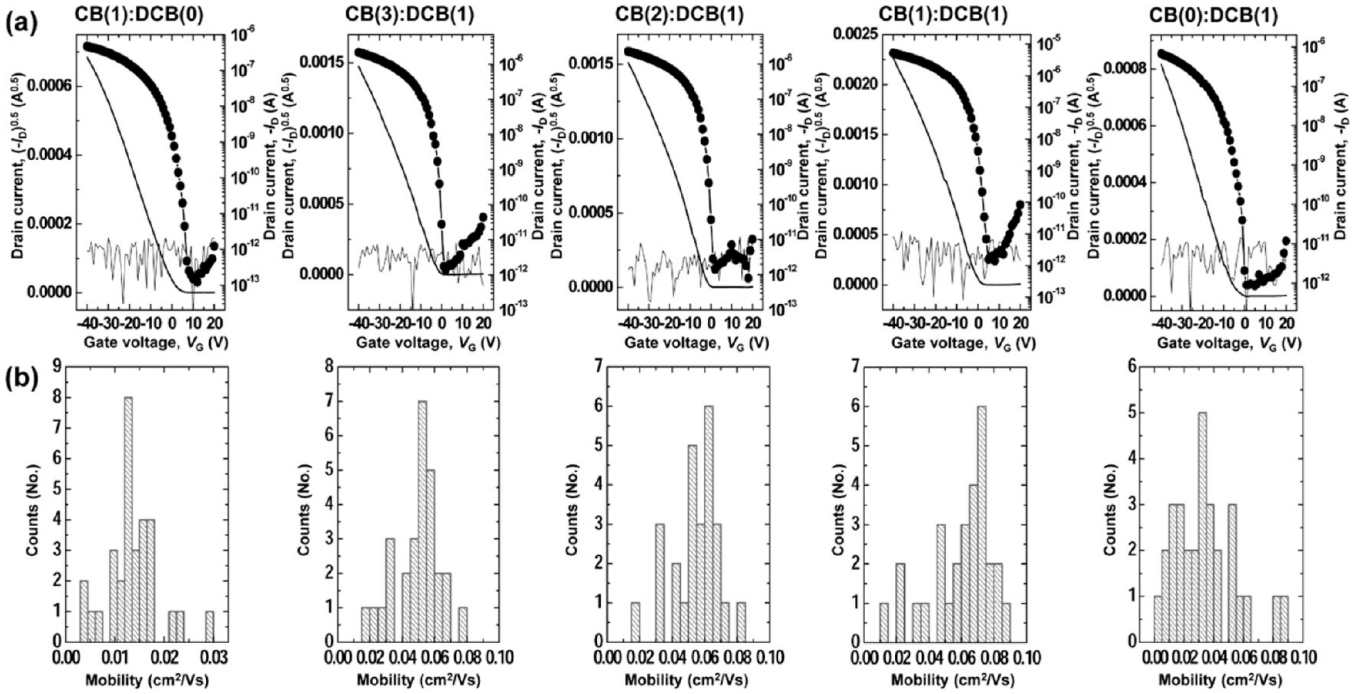

Figure 5. (a) $(-I_D)^{1/2}$ (left), $-I_D$ (right) versus the V_G characteristics of transistors based on TIPS_PEN active layers prepared from a variety of solvents. The light solid line shows the gate leakage current. (b) Summary of the field-effect mobilities measured from 29 transistors. The field-effect mobilities were calculated in the saturation regime, $V_D = -40$ V.

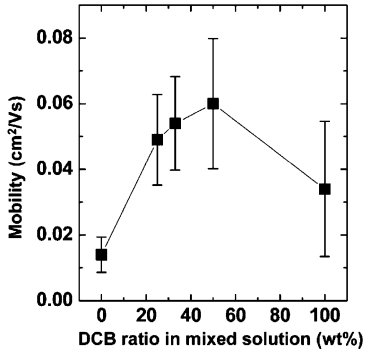

Figure 6. Changes in the average field-effect mobility of the transistors as a function of the DCB ratio in the mixed CB and DCB solvents.

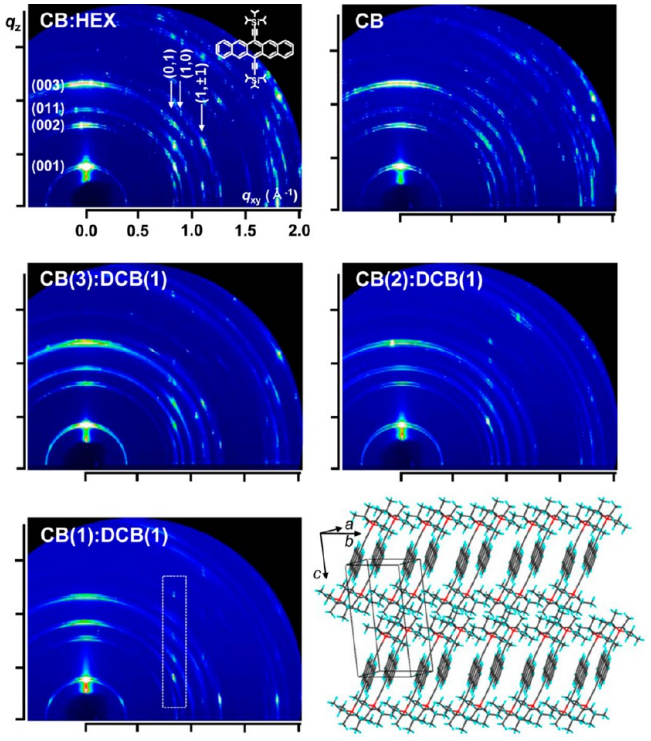

Figure 7. Two-dimensional grazing incidence X-ray diffraction (2D GIXD) patterns of the TIPS_PEN dots prepared from a variety of solvents. Chemical structures and molecular packing configurations of the TIPS_PEN films.

contact line remained pinned during the initial steps of the evaporation process. For this reason, the droplet size did not decrease significantly upon the addition of DCB, which has both a high boiling point and a high surface tension, as the minor solvent (Figure 4). These benefits induced TIPS_PEN crystallization at the pinned contact line whereas the added DCB induced slow evaporation of the solvent. Thus, regular dots and crystals with large sizes were obtained from CB/DCB solvent mixtures. The excellent electrical properties obtained from the mixed CB/DCB solvents were comparable with the properties of FETs obtained from spin-cast TIPS_PEN films,[41] indicating that the capillary pen patterning method was reliable and reproducible.

The precise molecular ordering and crystalline nature of the TIPS_PEN deposits were examined using 2D GIXD, as shown in Figure 7. Because the intensity of a 2D GIXD pattern is sensitive to the film thickness, the reflection intensity was not considered to contain meaningful information. The diffraction patterns for all cases contained both intense (00*l*) reflection patterns corresponding to a *c*-axis of 16.8 Å in the TIPS_PEN unit cell and a weak (011) peak along the q_z (out-of-plane) axis.[17,32] These results suggested that the TIPS_PEN molecules in the patterned deposits were mainly oriented such that the silyl groups were directed toward the substrate surface (the standing-up configuration, see the right bottom inset of Figure 7).

dx.doi.org/10.1021/am401698c | ACS Appl. Mater. Interfaces 2013, 5, 7838−7844

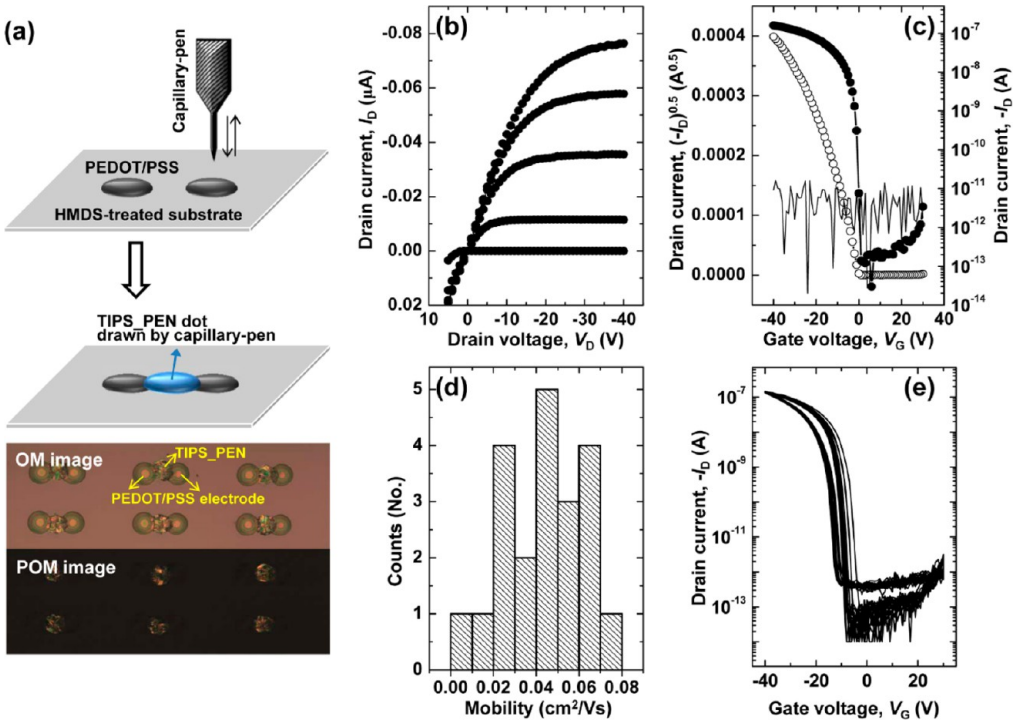

Figure 8. (a) Schematic diagram showing the procedure for fabricating a transistor using a TIPS_PEN active layer and PEDOT:PSS S/D electrodes. POM and OM images of the devices are also shown. (b and c) Output characteristics, $(-I_D)^{1/2}$ (left) and $-I_D$ (right), respectively, versus V_G for the transistors. The V_G for the output characteristics was changed from 0 V to −40 V with steps of −10 V. The solid line in part c shows the gate leakage current. (d) Summary of the field-effect mobilities of 21 transistors. (e) Sequential measurements collected from the transistors (20 times).

This crystal structure is advantageous for the transport of charge carriers because $\pi-\pi$ stacking along the lateral direction is maximized. The (011) reflections, however, displayed non-negligible intensities in all cases. These results suggest that the crystalline and morphological structures of the TIPS_PEN deposits were not optimized. The structures may potentially be improved by introducing a postannealing process, such as thermal or solvent-vapor annealing.[42−46]

It should be noted that the (0,1) and (1,0) reflections along the in-plane direction, which were indistinct for the CB:HEX and CB cases, become clearer for the cases of a CB:DCB mixed solution. These results suggest that the crystal perfection and ordering of the TIPS_PEN molecules along the in-plane direction were better in the CB:DCB system than in the CB:HEX and CB systems. Although the crystalline properties along the out-of-plane axis (q_z direction) were important to the FET device performance, the properties along the in-plane direction were more crucial because charge carrier transport proceeds laterally in the channel region between the source/drain electrodes.[9,47] Therefore, the differences between the (0,1) and (1,0) reflections may correlate with the enhanced field-effect mobilities observed in the FET devices in the CB:DCB mixed solvent cases.

The versatility of the capillary pen printing technique was evaluated by preparing integrated FET arrays on a silicon wafer with PEDOT:PSS electrodes and TIPS_PEN active layers. Figure 8a shows a schematic diagram of the fabrication process and a digital photograph of a device array with a bottom-contact structure. The fabricated array contained 253 TIPS_PEN FETs over a 2 cm × 2 cm area on the substrate, including 506 PEDOT:PSS and 253 TIPS_PEN dot arrays. Figure 8b and c shows the well-behaved output and transfer characteristics of the FETs, respectively. The average value and standard deviation of the field-effect mobility were 0.043 and 0.018 cm^2 V^{-1} s^{-1}, respectively, obtained from 21 devices, as indicated in Figure 8d. These values are relatively low compared to the best mobility of the solution-processed TIPS_PEN transistors. Considering the OFET devices composed of the fully printed active layer and S/D electrode, however, values of the mobility could be noticeable results. Stability tests involving sequential measurement showed that the device performances remained unchanged over time, demonstrating excellent device stability (Figure 8e). Consecutive printing processes are a prerequisite for OFET commercialization; therefore, the capillary pen system described here provides a versatile route to the mass production of OFETs.

4. CONCLUSIONS

In summary, we devised a facile method for fabricating organic semiconductor patterns using a capillary pen as a new printing method, which has the usefulness of the approach to the large-area printing and fabrication of organic transistors. The capillary pen printing method has several advantages: the method is simple and versatile. In addition, there are no restrictions on the patterned shapes, and the method may be tailored to a variety of substrates. We particularly examined the effects of the solvent on the morphological and structural properties of the capillary pen-drawn TIPS_PEN droplets. The solvent properties (i.e., the boiling point and surface tension) of the TIPS_PEN solution critically affected the final morphologies of the TIPS_PEN deposits. A mixed solvent containing equal masses of CB and DCB produced large crystals with an optimal pattern size. CB induced contact line pinning of the droplet, whereas DCB provided a long evaporation time that permitted crystallization of the TIPS_PEN molecules. On the other hand, contact line recession in a droplet formed from a single solvent with a high boiling point (i.e., DCB, TCB) resulted

in irregular patterns with a small dot size and a marginal crystal size. TIPS_PEN film deposits from mixed solvents containing equal masses of CB and DCB yielded the highest field-effect mobilities in FET applications. The structural basis for these results was investigated by characterizing the film structures using GIXD measurements. Finally, the semiconducting active layer and the S/D electrodes were fabricated using capillary pen deposition, demonstrating that our printing approach is quite promising for the fabrication of OFETs.

AUTHOR INFORMATION

Corresponding Author

*E-mail: hlee@hanbat.ac.kr.

Notes

The authors declare no competing financial interest.

ACKNOWLEDGMENTS

This work was supported by the Basic Science Research Program through the National Research Foundation of Korea (NRF) funded by the Ministry of Education, Science and Technology [2012-0003575].

REFERENCES

(1) Forrest, S. R. *Nature* **2004**, *428*, 911−918.
(2) Yan, H.; Chen, Z.; Zheng, Y.; Newman, C.; Quinn, J. R.; Dotz, F.; Kastler, M.; Facchetti, A. *Nature* **2009**, *457*, 679−686.
(3) Sirringhaus, H.; Kawase, T.; Friend, R. H.; Shimoda, T.; Inbasekaran, M.; Wu, W.; Woo, E. P. *Science* **2000**, *290*, 2123−2126.
(4) Berggren, M.; Nilsson, D.; Robinson, N. D. *Nat. Mater.* **2007**, *6*, 3−5.
(5) Nielsen, C. B.; Turbiez, M.; McCulloch, I. *Adv. Mater.* **2013**, *25*, 1859−1880.
(6) Qiu, L. Z.; Xu, Q.; Chen, M. J.; Wang, X. H.; Wang, X. H.; Zhang, G. B. *J. Mater. Chem.* **2012**, *22*, 18887−18892.
(7) Liu, S. H.; Wang, W. C. M.; Briseno, A. L.; Mannsfeld, S. C. E.; Bao, Z. N. *Adv. Mater.* **2009**, *21*, 1217−1232.
(8) Rivnay, J.; Mannsfeld, S. C.; Miller, C. E.; Salleo, A.; Toney, M. F. *Chem. Rev.* **2012**, *112*, 5488−5519.
(9) Braga, D.; Horowitz, G. *Adv. Mater.* **2009**, *21*, 1473−1486.
(10) Kang, I.; An, T. K.; Hong, J. A.; Yun, H. J.; Kim, R.; Chung, D. S.; Park, C. E.; Kim, Y. H.; Kwon, S. K. *Adv. Mater.* **2013**, *25*, 524−528.
(11) Tobjork, D.; Osterbacka, R. *Adv. Mater.* **2011**, *23*, 1935−1961.
(12) Moonen, P. F.; Yakimets, I.; Huskens, J. *Adv. Mater.* **2012**, *24*, 5526−5541.
(13) Cho, J. H.; Lee, J.; Xia, Y.; Kim, B.; He, Y.; Renn, M. J.; Lodge, T. P.; Frisbie, C. D. *Nat. Mater.* **2008**, *7*, 900−906.
(14) Noh, Y. Y.; Zhao, N.; Caironi, M.; Sirringhaus, H. *Nat. Nanotechnol.* **2007**, *2*, 784−789.
(15) Kim, S. H.; Hong, K.; Xie, W.; Lee, K. H.; Zhang, S.; Lodge, T. P.; Frisbie, C. D. *Adv. Mater.* **2013**, *25*, 1822−1846.
(16) Singh, M.; Haverinen, H. M.; Dhagat, P.; Jabbour, G. E. *Adv. Mater.* **2010**, *22*, 673−685.
(17) Lim, J. A.; Lee, W. H.; Lee, H. S.; Lee, J. H.; Park, Y. D.; Cho, K. *Adv. Funct. Mater.* **2008**, *18*, 229−234.
(18) Blaudeck, T.; Ersman, P. A.; Sandberg, M.; Heinz, S.; Laiho, A.; Liu, J.; Engquist, I.; Berggren, M.; Baumann, R. R. *Adv. Funct. Mater.* **2012**, *22*, 2939−2948.
(19) Minemawari, H.; Yamada, T.; Matsui, H.; Tsutsumi, J.; Haas, S.; Chiba, R.; Kumai, R.; Hasegawa, T. *Nature* **2011**, *475*, 364−367.
(20) James, D. T.; Kjellander, B. K. C.; Smaal, W. T. T.; Gelinck, G. H.; Combe, C.; McCulloch, I.; Wilson, R.; Burroughes, J. H.; Bradley, D. D. C.; Kim, J. S. *ACS Nano* **2011**, *5*, 9824−9835.
(21) Madec, M. B.; Smith, P. J.; Malandraki, A.; Wang, N.; Korvink, J. G.; Yeates, S. G. *J. Mater. Chem.* **2010**, *20*, 9155−9160.
(22) Carlson, A.; Bowen, A. M.; Huang, Y.; Nuzzo, R. G.; Rogers, J. A. *Adv. Mater.* **2012**, *24*, 5284−5318.
(23) Qin, D.; Xia, Y. N.; Whitesides, G. M. *Nat. Protoc.* **2010**, *5*, 491−502.
(24) Lee, J. N.; Park, C.; Whitesides, G. M. *Anal. Chem.* **2003**, *75*, 6544−6554.
(25) Voigt, M. M.; Guite, A.; Chung, D. Y.; Khan, R. U. A.; Campbell, A. J.; Bradley, D. D. C.; Meng, F. S.; Steinke, J. H. G.; Tierney, S.; McCulloch, I.; Penxten, H.; Lutsen, L.; Douheret, O.; Manca, J.; Brokmann, U.; Sonnichsen, K.; Hulsenberg, D.; Bock, W.; Barron, C.; Blanckaert, N.; Springer, S.; Grupp, J.; Mosley, A. *Adv. Funct. Mater.* **2010**, *20*, 239−246.
(26) Vornbrock, A. D.; Sung, D. V.; Kang, H. K.; Kitsomboonloha, R.; Subramanian, V. *Org. Electron.* **2010**, *11*, 2037−2044.
(27) Schmidt, G. C.; Bellmann, M.; Meier, B.; Hambsch, M.; Reuter, K.; Kempa, H.; Hubler, A. C. *Org. Electron.* **2010**, *11*, 1683−1687.
(28) Hambsch, M.; Reuter, K.; Kempa, H.; Hubler, A. C. *Org. Electron.* **2012**, *13*, 1989−1995.
(29) Sparrowe, D.; Baklar, M.; Stingelin, N. *Org. Electron.* **2010**, *11*, 1296−1300.
(30) Kang, H.; Kitsomboonloha, R.; Jang, J.; Subramanian, V. *Adv. Mater.* **2012**, *24*, 3065−3069.
(31) Lim, J. A.; Lee, H. S.; Lee, W. H.; Cho, K. *Adv. Funct. Mater.* **2009**, *19*, 1515−1525.
(32) Kim, D. H.; Lee, D. Y.; Lee, H. S.; Lee, W. H.; Kim, Y. H.; Han, J. I.; Cho, K. *Adv. Mater.* **2007**, *19*, 678−682.
(33) Payne, M. M.; Parkin, S. R.; Anthony, J. E.; Kuo, C. C.; Jackson, T. N. *J. Am. Chem. Soc.* **2005**, *127*, 4986−4987.
(34) Giri, G.; Verploegen, E.; Mannsfeld, S. C. B.; Atahan-Evrenk, S.; Kim, D. H.; Lee, S. Y.; Becerril, H. A.; Aspuru-Guzik, A.; Toney, M. F.; Bao, Z. A. *Nature* **2011**, *480*, 504−508.
(35) Lim, J. A.; Lee, W. H.; Kwak, D.; Cho, K. *Langmuir* **2009**, *25*, 5404−5410.
(36) Petsi, A. J.; Burganos, V. N. *Phys. Rev. E* **2005**, *72*, 047301−047304.
(37) Salleo, A. *Mater. Today* **2007**, *10*, 38−45.
(38) Briseno, A. L.; Mannsfeld, S. C.; Ling, M. M.; Liu, S.; Tseng, R. J.; Reese, C.; Roberts, M. E.; Yang, Y.; Wudl, F.; Bao, Z. *Nature* **2006**, *444*, 913−917.
(39) Nakayama, K.; Hirose, Y.; Soeda, J.; Yoshizumi, M.; Uemura, T.; Uno, M.; Li, W. Y.; Kang, M. J.; Yamagishi, M.; Okada, Y.; Miyazaki, E.; Nakazawa, Y.; Nakao, A.; Takimiya, K.; Takeya, J. *Adv. Mater.* **2011**, *23*, 1626−1629.
(40) Deegan, R. D. *Phys. Rev. E* **2000**, *61*, 475−485.
(41) Park, S. K.; Jackson, T. N.; Anthony, J. E.; Mourey, D. A. *Appl. Phys. Lett.* **2007**, *91*, 063514−063516.
(42) Lee, W. H.; Kim, D. H.; Cho, J. H.; Jang, Y.; Lim, J. A.; Kwak, D.; Cho, K. *Appl. Phys. Lett.* **2007**, *91*, 092105−092107.
(43) Dickey, K. C.; Smith, T. J.; Stevenson, K. J.; Subramanian, S.; Anthony, J. E.; Loo, Y. L. *Chem. Mater.* **2007**, *19*, 5210−5215.
(44) Verploegen, E.; Miller, C. E.; Schmidt, K.; Bao, Z. N.; Toney, M. F. *Chem. Mater.* **2012**, *24*, 3923−3931.
(45) De Luca, G.; Treossi, E.; Liscio, A.; Mativetsky, J. M.; Scolaro, L. M.; Palermo, V.; Samori, P. *J. Mater. Chem.* **2010**, *20*, 2493−2498.
(46) Miller, S.; Fanchini, G.; Lin, Y. Y.; Li, C.; Chen, C. W.; Su, W. F.; Chhowalla, M. *J. Mater. Chem.* **2008**, *18*, 306−312.
(47) Facchetti, A. *Mater. Today* **2007**, *10*, 28−37.